MOVEMENT OF GROUND WATER IN CONVERGING AQUIFER

By Allen T. Hjelmfelt Jr.,[1] Member, ASCE, and Zhanzhong Pi[2]

ABSTRACT: An analytical solution for regional flow in a converging or wedge-shaped aquifer is given. Darcy's law and the continuity equation, expressed in cylindrical coordinates, were solved for flow in a vertical cross section of a two-dimensional aquifer. The lower horizontal boundary and the vertical boundaries at $r = 0$ and $r = a$ are no-flow boundaries. The upper horizontal boundary is a prescribed head consisting of a linear increase with radius onto which is superimposed a sine wave. In plan view, the streamlines are radially convergent. The converging system shows a concentration of streamlines near the divide and a spreading of streamlines near the apex due to the prescribed potential on the upper boundary that limits the rate of water movement toward the apex. The effect of relief on local flow systems is limited, especially in the region near the valley bottom.

INTRODUCTION

Knowledge of patterns of ground-water flow is needed to understand and predict the movement of agricultural nutrients and pesticides through the soil profile and the ground-water system of an upland watershed. Upland watersheds are often best described in plan view as a sector of a circle rather than a rectangular element. Shallow aquifers underlying these upland watersheds often conform to the surface boundaries. Surface-water hydrologists have noted this difference in geometry and have developed appropriate kinematic wave models to describe the surface runoff. They have found the response of a converging watershed to be quite different from the response of a rectangular watershed. Notable are the works of Woolhiser (1969), Woolhiser et al. (1971), Singh and Woolhiser (1976), and Singh and Shelbourne (1979).

Ground-water flow can be described by a diffusion equation, whereas surface flow is described by a wave equation. As a result, solutions for surface flow are not directly applicable to the ground-water problem. One can infer, however, that significant differences will be exhibited in the ground-water flow when comparing flow in a rectangular aquifer with flow in a converging aquifer. Numerical modeling of such watersheds, using general modeling packages, is best done using a variable grid spacing. Prickett and Lonnquist (1971) point out, however, that definition of the variable grid spacing is not necessarily obvious.

A theoretical analysis of a two-dimensional regional aquifer was described by Tóth (1962, 1963). His work has been widely used as a conceptual basis for describing expected behavior (Wang and Anderson 1982) and for interpreting observed behavior of ground water in small watersheds (Pionke et al. 1986). More general research, using both analytical and numerical

[1]Res. Hydr. Engr., USDA-Agric. Res. Service, Agric. Engrg. Bldg., Univ. of Missouri, Columbia, MO 65211.

[2]Grad. Student, Agric. Engrg. Dept., Agric. Engrg. Bldg., Univ. of Missouri, Columbia, MO.

Note. Discussion open until September 1, 1993. To extend the closing date one month, a written request must be filed with the ASCE Manager of Journals. The manuscript for this paper was submitted for review and possible publication on October 30, 1991. This paper is part of the ***Journal of Irrigation and Drainage Engineering***, Vol. 119, No. 2, March/April, 1993. ©ASCE, ISSN 0733-9437/93/0002-0312/$1.00 + $.15 per page. Paper No. 2894.

solutions, for regional ground-water movement in rectangular, three-dimensional, nonhomogeneous, anisotropic basins was done by Freeze and Witherspoon (1966, 1967, 1968). This work is not, however, directly applicable to converging aquifers. An analytic solution, similar to that of Tóth (1963), would be helpful in interpreting ground-water movement in converging upland watersheds and will help in defining the grid spacing for numerical models.

Basic Assumptions

Following Tóth (1963) and Freeze and Witherspoon (1966), it is assumed that there exists a hydrologic unit (the ground-water basin) that contains the entire flow paths followed by the ground recharging the basin. It is bounded on the bottom by an impermeable layer and on the sides by streamlines across which there is no flow. These side boundaries describe a pie-shaped wedge in plan view. The formation above the horizontal, impermeable lower boundary is homogeneous and isotropic. The hydrologic unit is bounded on the top by the water table. This upper boundary of the saturated flow system is known and, on a long-term average basis, can be treated as steady state. In the analytical solution described here the upper boundary condition is specified along a horizontal plane, and the potential representing the water table is specified along this plane. Freeze and Witherspoon (1966) gave an extensive defense of this assumption. In the work that follows, radial symmetry is also assumed.

Mathematical Model

Application of Darcy's law and the continuity equation for steady, axisymmetrical, homogeneous, and isotropic flow results in the following form of the Laplace equation

$$\frac{\partial^2 h}{\partial r^2} + \frac{1}{r}\frac{\partial h}{\partial r} + \frac{\partial^2 h}{\partial z^2} = 0 \quad \ldots\ldots\ldots\ldots\ldots\ldots\ldots\ldots\ldots\ldots\ldots\ldots\ldots\ldots\ldots\ldots (1)$$

where h = hydraulic head at a given point; r = radial coordinate; and z = vertical coordinate. Fig. 1 depicts the geometry under consideration.

The boundary conditions are: The radial velocity is zero at zero radius

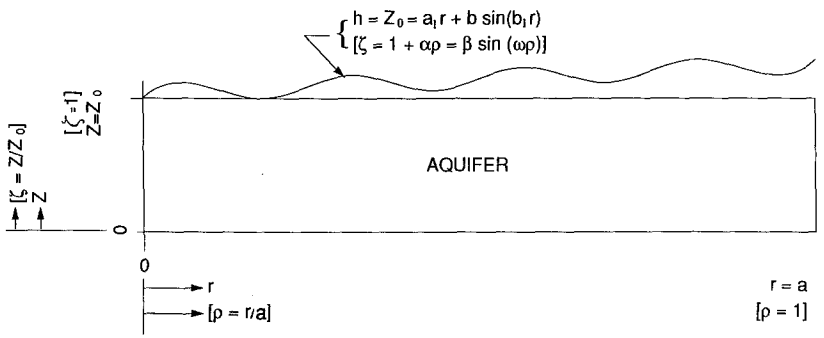

FIG. 1. Side View. Aquifer is Wedge-Shaped in Plan View

$$v_r|_{r=0} = K\frac{\partial h}{\partial r}|_{r=0} = 0 \qquad \text{for } 0 \le z \le z_0 \quad \ldots\ldots (2)$$

the radial velocity is zero at the outer boundary, $r = a$

$$v_r|_{r=a} = K\frac{\partial h}{\partial r}|_{r=a} = 0 \qquad \text{for } 0 \le z \le z_0 \quad \ldots\ldots (3)$$

and the vertical velocity is zero along the impermeable bottom boundary, $z = 0$

$$v_z|_{z=0} = K\frac{\partial h}{\partial z}|_{z=0} = 0 \qquad \text{for } 0 \le r \le a \quad \ldots\ldots (4)$$

also, due to the known, quasi–steady-state water table, the potential at elevation $z = z_0$ is given by

$$h|_{z=z_0} = z_0 + a_1 r + b\sin(b_1 r) \qquad \text{for } 0 \le r \le a \quad \ldots\ldots (5)$$

where v_r = the radial velocity of the ground water; v_z = the vertical velocity of the ground water; K = hydraulic conductivity; z_0 = the depth to the horizontal impermeable boundary; $a_1 = \tan\alpha_1$, α_1 = angle of slope; b = amplitude of the sine wave; $b_1 = 2\pi/\lambda$, which is the frequency of the sine wave; and λ = the period of the sine wave. The boundary condition at $z = z_0$ [(5)] is the same as that used by Tóth (1963). It was used to facilitate comparison with the rectangular case. The term a_1 was considered by Tóth (1963) to represent the general slope of the valley. The sine term was considered to describe topographic relief and was interpreted as representing local stream systems. This pattern of local stream systems is not typical for converging upland agricultural watersheds. Use of terrace systems for erosion control is common, however, and infiltration of water stored behind the terraces can lead to a potential similar to that described by (5).

It is convenient to express these relations in nondimensional form by using $\eta = h/z_0$, $\rho = r/a$, and $\zeta = z/z_0$. The basic equation [(1)] becomes

$$\frac{\partial^2\eta}{\partial\rho^2} + \frac{1}{\rho}\frac{\partial\eta}{\partial\rho} + \frac{a^2}{z_0^2}\frac{\partial^2\eta}{\partial\zeta^2} = 0 \quad \ldots\ldots (6)$$

with boundary conditions

$$\frac{\partial\eta}{\partial\rho}|_{\rho=0} = 0 \quad \ldots\ldots (7)$$

$$\frac{\partial\eta}{\partial\rho}|_{\rho=1} = 0 \quad \ldots\ldots (8)$$

$$\frac{\partial\eta}{\partial\zeta}|_{\zeta=0} = 0 \quad \ldots\ldots (9)$$

$$\eta|_{\zeta=1} = 1 + \alpha\rho + \beta\sin(\omega\rho) \quad \ldots\ldots (10)$$

where $\alpha = a_1/z_0$; $\beta = b/z_0$; and $\omega = b_1 a = 2\pi a/\lambda$.

The general solution of (6) with boundary conditions (7), (8), and (9) can be determined using the method of separation of variables following Carslaw and Jaeger (1959). The solution of the radial portion of the equation is in terms of Bessel functions, whereas the solution of the z portion of the

equation is in terms of hyperbolic functions. The general solution can be written in the following form:

$$\eta = \sum_{n=0}^{\infty} C_n \cosh\left(\frac{z_0}{a}\lambda_n\zeta\right) J_0(\lambda_n\rho) \quad \ldots\ldots (11)$$

where $J_0(\lambda_n\rho)$ = the zero-order Bessel function. The λ_n are zeros of the first-order Bessel function, that is

$$J_1(\lambda_n) = 0 \quad \ldots\ldots (12)$$

Abramowitz and Stegun (1964) provide the following expansion by which values of λ_n can be determined

$$\lambda_n \approx \nu - \frac{3}{8\nu} + \frac{12}{(8\nu)^3} - \frac{9452.8}{(8\nu)^5} + \frac{11079696.46}{(8\nu)^7} + \cdots \quad \ldots\ldots (13)$$

where $\nu = (n + 1/4)\pi$; and $1 \leq n < \infty$.

The constants C_n are found using the upper boundary condition [(10)]. Eq. (11) is written for $\zeta = 1$ and equated to the boundary condition [(10)]. Both sides of the equation are multiplied by $\rho J_0(\lambda_k\rho)\, d\rho$ and integrated. The result is

$$C_n = \frac{A_n + B_n}{\cosh\left(\frac{\lambda_n z_0}{a}\right)} \quad \ldots\ldots (14)$$

where

$$A_n = \frac{2\alpha \int_0^1 \rho^2 J_0(\lambda_n\rho)\, d\rho}{[J_0(\lambda_n)]^2} \quad \ldots\ldots (15)$$

and

$$B_n = \frac{2\beta \int_0^1 \rho \sin(\omega\rho) J_0(\lambda_n\rho)\, d\rho}{[J_0(\lambda_n)]^2} \quad \ldots\ldots (16)$$

Let

$$D_n = -(A_n + B_n) \quad \ldots\ldots (17)$$

so that (11) can be written

$$\eta = 1 + \sum_{n=1}^{\infty} D_n \left[1 - \frac{\cosh\left(\frac{\lambda_n z_0 \zeta}{a}\right)}{\cosh\left(\frac{\lambda_n z_0}{a}\right)} J_0(\lambda_n\rho)\right] \quad \ldots\ldots (18)$$

The no-flow boundary conditions [(7), (8), and (9)] determine the form of solution of the problem and the characteristic values λ_n, whereas the boundary condition [(10)] that specifies the configuration of water table determines the ground-water flow pattern. The flow pattern will vary with

the slope α and the sine curve parameters β and ω. The coefficients A_n and B_n represent the effect of slope and sine curve, respectively.

For homogeneous, isotropic, potential flow, nondimensional velocities can be determined using Darcy's law. These nondimensional velocities are defined as

$$v_\rho = \frac{v_r}{k} = \frac{z_0}{a}\frac{\partial \eta}{\partial \rho} \quad \ldots\ldots (19)$$

$$v_\zeta = \frac{v_z}{k} = \frac{\partial \eta}{\partial \zeta} \quad \ldots\ldots (20)$$

For an axisymmetrical potential flow, the Stokes stream function is defined as

$$d[\psi(r, z)] = r(v_z\, dr - v_r\, dz) \quad \ldots\ldots (21)$$

The relation for the stream function is obtained by dividing (21) by $k \cdot a \cdot z_0$, and substituting (19) and (20) into the result. This leads to the nondimensional form

$$d[\psi(\rho, \zeta)] = \rho\left[\frac{a}{z_0}\frac{\partial \eta}{\partial \zeta}\, d\rho - \frac{z_0}{a}\frac{\partial \eta}{\partial \rho}\, d\zeta\right] \quad \ldots\ldots (22)$$

Then

$$\frac{\partial \psi}{\partial \rho} = \left(\frac{a}{z_0}\right)\rho\frac{\partial \eta}{\partial \zeta} \quad \ldots\ldots (23)$$

$$\frac{\partial \psi}{\partial \zeta} = -\left(\frac{z_0}{a}\right)\rho\frac{\partial \eta}{\partial \rho} \quad \ldots\ldots (24)$$

Upon integration, the nondimensional stream function is

$$\psi = \sum_{n=1}^{\infty}(A_n + B_n)\frac{\sinh\left(\frac{\lambda_n z_0 \zeta}{a}\right)}{\cosh\left(\frac{\lambda_n z_0}{a}\right)}\rho J_1(\lambda_n \rho) \quad \ldots\ldots (25)$$

where ψ = nondimensional stream function, and J_1 = first-order Bessel function.

Numerical Results

To analyze the effect of the converging aquifer (17) and (18) were evaluated for the same examples selected by Tóth (1963). Zeros of the first-order Bessel function were evaluated using (12). The hyperbolic-cosine Bessel function series [(18)] is not rapidly convergent, so more than 100 terms were regularly summed to attain the desired accuracy. The results are displayed graphically in Figs. 2–10.

The nondimensional hydraulic head, η, is plotted as dashed lines. Streamlines, determined using (25), are plotted as solid lines. Three aspect ratios (z_0/a) 0.05, 0.25, and 0.50 were considered. These correspond to shallow,

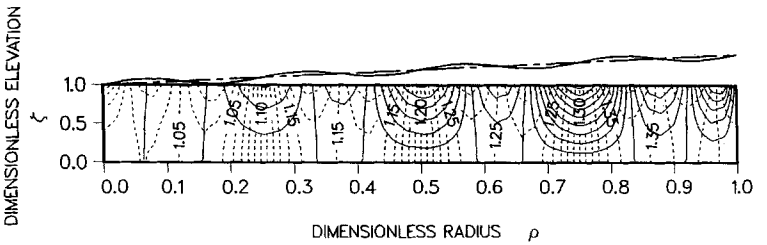

FIG. 2. Flow System for Aspect Ratio z_0/a = 0.05; Slope a_1/a = 0.02; and Amplitude b/a = 0.0025

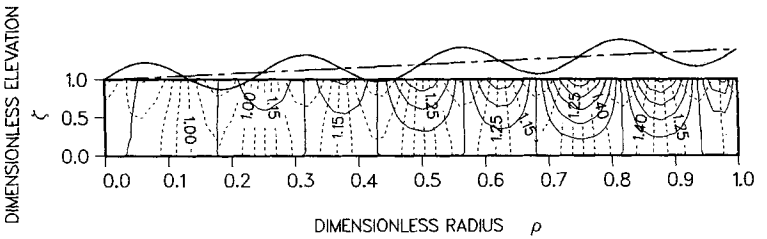

FIG. 3. Flow System for Aspect Ratio z_0/a = 0.05; Slope a_1/a = 0.02; and Amplitude b/a = 0.01

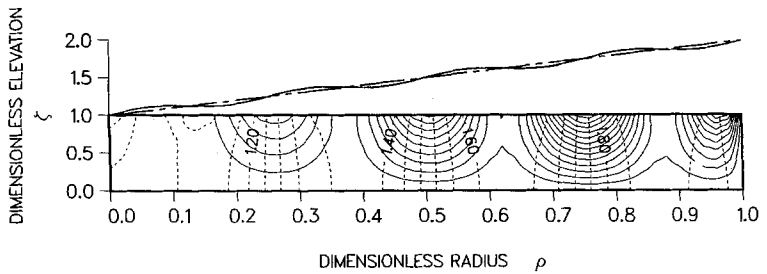

FIG. 4. Flow System for Aspect Ratio z_0/a = 0.05; Slope a_1/a = 0.05; and Amplitude b/a = 0.0025

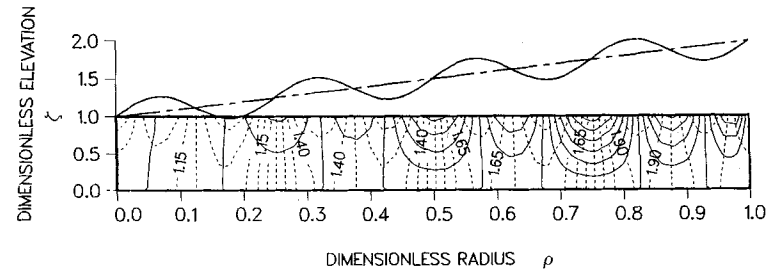

FIG. 5. Flow System for Aspect Ratio z_0/a = 0.05; Slope a_1/a = 0.05; and Amplitude b/a = 0.01

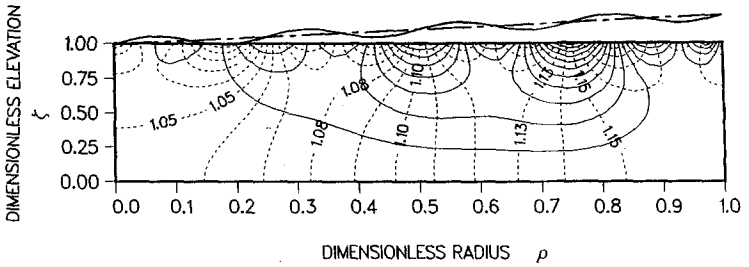

FIG. 6. Flow System for Aspect Ratio z_0/a = 0.25; Slope a_1/a = 0.05; and Amplitude b/a = 0.01

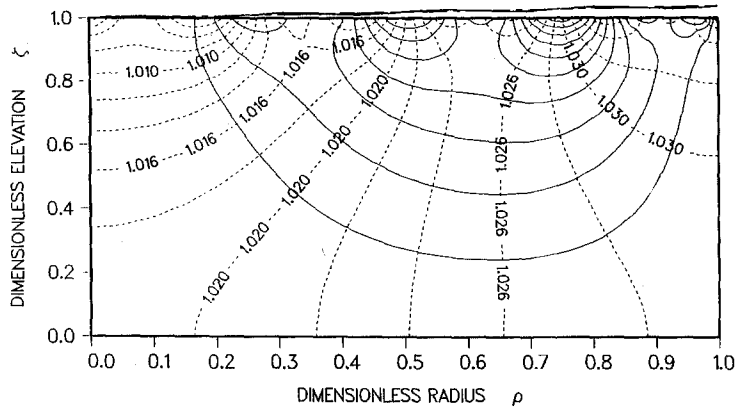

FIG. 7. Flow System for Aspect Ratio z_0/a = 0.50; Slope a_1/a = 0.02; and Amplitude b/a = 0.0025

moderate, and thick saturated zones and to the aspect ratios used by Tóth (1963). For the water table configuration, that is, the upper boundary condition, two slopes ($a_1/a = \alpha z_0/a = 0.02$ and 0.05) and two relative amplitudes ($b/a = \beta a/z_0 = 0.0025$ and 0.01) were used. Again, these correspond with the values used by Tóth.

Three different flow systems are apparent, as they were for Tóth (1963). These flow systems are as follows.

1. A local system in which flow has its recharge at a topographic high and its discharge at an adjacent topographic low. Streamlines originate in the positive portion of the sine curve and terminate in the adjacent negative portion. Local flow systems are apparent in each of the geometries analyzed.
2. Intermediate systems are those in which streamlines span one or more topographic lows. Intermediate flow systems are apparent on the moderate and thick saturated flow geometries.
3. Regional systems are those in which the recharge area is at the divide, where $r = a$, and the discharge region is at the outlet of the watershed, where $r = 0$. Mathematically, one streamline should follow the boundary of the aquifer, and so it would define a regional flow. Regional flow is very limited in the thin saturated zone case, though regional flow can be expected in Fig. 4.

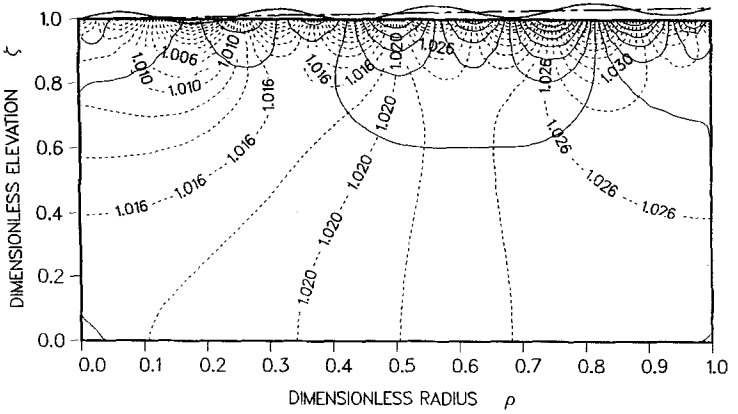

FIG. 8. Flow System for Aspect Ratio z_0/a = 0.50; Slope a_1/a = 0.02; and Amplitude b/a = 0.01

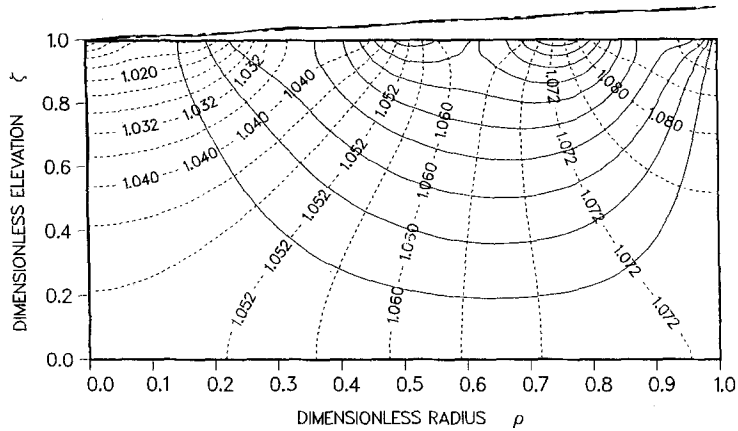

FIG. 9. Flow System for Aspect Ratio z_0/a = 0.50; Slope a_1/a = 0.05; and Amplitude b/a = 0.0025

The effect of thickness of the saturated layer on the flow pattern can be analyzed by considering Figs. 5, 6, and 10. All parameters are held constant except the aspect ratio. For the shallow case (Fig. 5) the only prevalent flow system is local. For the moderate and thick aspect ratios, intermediate and regional systems appear. In general, thicker saturated layers lead to greater flow in the regional system.

The influence of general topographic slope is given by $a_1/a = \alpha z_0/a$, whereas topographic relief is indicated by the amplitude of the sine wave, $\beta z_0/a$. The influence of slope can be analyzed by comparing Fig. 2 with Fig. 4 and Fig. 7 with Fig. 9. Increases in slope result in a greater potential gradient, eventually overcoming the local gradient caused by the sine wave. This leads to a breakdown of the local flow and to an increased significance for the intermediate and regional flow systems. Conversely, an increase in the topographic relief tends to enhance the local flow system to the detriment of the intermediate and regional systems. This is demonstrated in Figs. 4

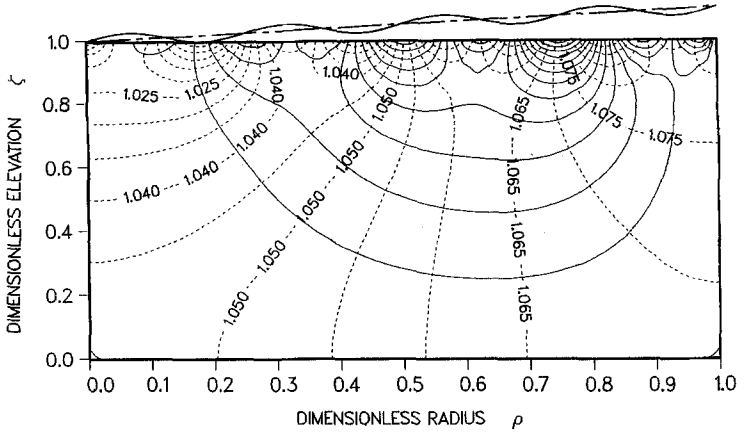

FIG. 10. Flow System for Aspect Ratio z_0/a = 0.50; Slope a_1/a = 0.50; and Amplitude b/a = 0.01

and 5. Obviously, the amplitude, β, and frequency, ω, of the sine curve determine the local flow system of the ground-water movement, and the slope α determines the regional flow system of the ground-water movement.

These observations agree, in general, with those of Tóth (1963). There are, however, significant differences. The flow pattern is distorted from that of Tóth (1963) with the streamlines closer together at the divide ($r = a$) of the convergent aquifer, but toward the apex the streamlines are spread farther apart. These differences, which are more apparent with the moderate and thick saturated zones and with steeper valley slopes, suggest that the radial distance over which regional recharge occurs is relatively small and the radial distance over which regional discharge occurs is relatively large. In the Tóth (1963) case, for regional flow, the recharge and discharge intervals are the same. This occurs because, in plan view, the streamlines are straight and parallel, and the areas over which recharge and discharge occur must be equal to satisfy continuity. The areas must also be equal in the radially covergent case in order to satisfy continuity. In this case, the boundary between equal areas is $r/a = 2^{-0.5} = 0.707$. This forces a closer spacing of streamlines in the regional recharge region than in the regional discharge region.

In the examples with the moderate and thick saturated zones (Figs. 6–10), the intermediate flow system is more highly developed than in the Tóth (1963) case. In addition, this intermediate flow system is displaced upslope. This contributes to the expanded discharge distance.

These general observations can also be interpreted in terms of upland, terraced watersheds. Terrace systems that impound water can result in the equivalent of topographic relief described by the sine wave. A detrimental effect of a local flow system is seepage at the toe of the terrace, a problem requiring installation of a drainage system. A regional flow system may maintain baseflow in a stream draining the watershed. The bank seepage producing this flow and changes in that seepage can serve to destabilize the bank leading to increased soil loss.

Conclusions

This analysis indicates that the gross flow patterns are similar for the Tóth (1963) case and for converging aquifers. There are, however, distinct differences. The flow patterns for the converging systems show a concentration of streamlines near the divide and a spreading of streamlines near the apex. This is due to the prescribed potential on the upper boundary that limits the rate of water movement toward the apex.

Results for the converging aquifer indicate that the effect of relief on the local flow system is decreased near the valley bottom compared to that for the rectangular aquifer. For larger aspect ratios, the intermediate flow system is more highly developed, and it is displaced upslope.

Acknowledgment

The writers gratefully acknowledge the helpful comments of two anonymous reviewers that enhanced the paper.

Appendix I. References

Abramowitz, M., and Stegun, I. A. (1964). *Handbook of mathematical functions with formulas, graphs, and mathematical tables*. Nat. Bureau of Standards, Appl. Math Series 55, U. S. Government Printing Office, Washington, D.C.

Carslaw, H. S., and Jaeger, J. C. (1959). *Conduction of Heat in Solids*, Oxford Univ. Press, Oxford, England.

Freeze, R. A., and Witherspoon, P. A. (1966). "Theoretical analysis of regional groundwater flow: 1. Analysis and numerical solutions to the mathematical model." *Water Resour. Res.*, 2(4), 641–656.

Freeze, R. A., and Witherspoon, P. A. (1967). "Theoretical analysis of regional groundwater flow: 2. Effect of water-table configuration and subsurface permeability variation." *Water Resour. Res.*, 3(2), 623–634.

Freeze, R. A., and Witherspoon, P. A. (1968). "Theoretical analysis of regional groundwater flow: 3. Quantitative interpretations." *Water Resour. Res.*, 4(3), 581–590.

Pionke, H. B., Schnabel, R. R., Hoover, J. R., Gburek, W. J., Urban, J. B., and Rogowski, A. S. (1986). "Mahantango Creek Watershed—Fate and transport of water and nutrients." *Watershed Research Perspectives*, D. L. Correll, ed., Smithsonian Inst. Press, Washington, D.C., 108–134.

Singh, V. P., and Shelbourne, K. L. (1979). "Use of watershed topography to determine converging overland flow parameters." *J. Inst. Engrs. (India)*, 59(6), 388–393.

Singh, V. P., and Woolhiser, D. A. (1976). "A nonlinear kinematic wave model for watershed surface runoff." *J. Hydrol.*, 31, 221.

Tóth, J. (1962). "A theory of groundwater movement in small drainage basins in central Alberta, Canada." *J. Geophysical Res.*, 67(11), 4375–4387.

Tóth, J. (1963). "A theoretical analysis of groundwater flow in small drainage basin." *J. Geophysical Res.*, 68(16), 4795–4812.

Wang, H. F., and Anderson, M. P. (1982). *Introduction to groundwater modeling*. W. H. Freeman and Co., New York, N.Y.

Woolhiser, D. A. (1969). "Overland flow on a converging surface." *Trans. Am. Soc. Agr. Engr.*, 12(4), 460–462.

Woolhiser, D. A., Holland, M. E., Smith, G. L., and Smith, R. E. (1971). "Experimental investigation of converging overland flow." *Trans. Am. Soc. Agr. Engr.*, 14(4), 684–687.

Appendix II. Notation

The following symbols are used in this paper:

a = radius of outer boundary;
a_1 = $\tan(\alpha_1)$;

b = amplitude of sine wave;
b_1 = $2\pi/\lambda$, frequency of sine wave;
h = hydraulic head;
J_0 = zero-order Bessel function;
J_1 = first-order Bessel function;
K = hydraulic conductivity;
r = radial coordinate;
v_r = radial velocity;
v_z = axial velocity;
z = axial or vertical coordinate;
z_0 = thickness of aquifer;
α = a_1/z_0;
α_1 = angle of slope;
β = b/z_0;
ζ = z/z_0;
η = h/z_0;
λ = period of sine wave;
λ_n = zeros of first-order Bessel function;
ρ = r/a;
ψ = nondimensional stream function; and
ω = $b_1 a = 2\pi a/\lambda$.